

L-M-A-L

TECHNICAL NOTES

NATIONAL ADVISORY COMMITTEE FOR AERONAUTICS

No. 708

A SIMPLIFIED METHOD FOR THE CALCULATION OF
AIRFOIL PRESSURE DISTRIBUTION

By H. Julian Allen
Langley Memorial Aeronautical Laboratory

Washington
May 1939



NATIONAL ADVISORY COMMITTEE FOR AERONAUTICS

TECHNICAL NOTE NO. 708

A SIMPLIFIED METHOD FOR THE CALCULATION OF
AIRFOIL PRESSURE DISTRIBUTION

By H. Julian Allen

SUMMARY

A method is presented for the rapid calculation of the pressure distribution over an airfoil section when the normal-force distribution and the pressure distribution over the "base profile" (i.e., the profile of the same airfoil were the camber line straight and the resulting airfoil at zero angle of attack) are known. This note is intended as a supplement to N.A.C.A. Reports Nos. 631 and 634 wherein methods are presented for the calculation of the normal-force distribution over plain and flapped airfoils, respectively, but not of the pressures on the individual surfaces.

Base-profile pressure-coefficient distributions for the usual N.A.C.A. family of airfoils, which are also suitable for several other commonly employed airfoils, are included in tabular form. With these tabulated base-profile pressures and the computed normal-force distributions, pressure distributions adequate for most engineering purposes can be obtained.

INTRODUCTION

A method is given in reference 1 for computing the chordwise pressure distribution over both the upper and the lower surfaces of an airfoil. In this method, a perfect nonviscous fluid was assumed and, consequently, the agreement between the integrated forces and moments and those obtained from experimental observations was in many cases inadequate. In the work reported in reference 2, the effect of viscosity was accounted for by an adjustment of the mean camber line of the airfoil and the agreement was improved. Both methods, however, are too laborious for practical use even though the results might be considered adequate for design purposes.

A subsequent analysis of theory and experimental data (references 3 and 4) resulted in a series of charts whereby the normal-force distributions, but not the pressures on the individual surfaces, could be obtained for ordinary airfoils and airfoils with flaps. In this method, the magnitudes of the various component distributions that are added to obtain the normal-force distribution are determined from experimental force and moment coefficients. When the calculated normal-force distribution is integrated, it then yields normal-force and moment coefficients that must agree in magnitude with the corresponding experimental coefficients.

The present paper, which is a supplement to references 3 and 4, gives a method of utilizing the calculated normal-force distribution to obtain the pressures on the individual surfaces of an airfoil. Again, the resulting pressure distributions when integrated must yield normal-force and moment coefficients that agree with those obtained by experiment.

This method requires, in addition to a knowledge of the chordwise normal-force distribution over the airfoil section (as may be obtained from references 3 and 4), the pressure distribution over the "base profile" of the airfoil section (i.e., the profile of the same airfoil were the camber line straight and the resulting airfoil at zero angle of attack). The method is applicable, to date, to normal airfoils and to airfoils with plain trailing-edge flaps. The base-profile pressure distributions for the N.A.C.A. family of airfoils (as well as for the Clark Y and the Gottingen 398) calculated by the method of reference 1 are given in this report.

THEORY OF THE METHOD

Let it be assumed that the chordwise distribution of the filaments of the bound vortices within an airfoil section are located along the mean camber line and that the curvature of the mean camber line is slight so that the induced velocities on the upper and the lower surfaces at any given distance, x , behind the leading edge of the airfoil are equal in magnitude but opposite in sign.

The velocities on the upper and the lower surfaces of the airfoil at any point, x , behind the leading edge are, respectively,

$$\left. \begin{aligned} u_U &= u' + \Delta u \\ u_L &= u' - \Delta u \end{aligned} \right\} \quad (1)$$

where Δu is the induced velocity and u' is assumed to be the velocity that the base profile would experience at the point x behind the leading edge under the same stream conditions.

If p_f be designated as the surface pressure at x on the base profile, then, by Bernoulli's equation,

$$p_f = \frac{\rho U^2}{2} - \frac{\rho (u')^2}{2}$$

or

$$p_f = q - q \left(\frac{u'}{U} \right)^2$$

Hence

$$\frac{u'}{U} = \sqrt{1 - P_f}, \quad u' = U \sqrt{1 - P_f} \quad (2)$$

where U is the stream velocity and P_f is the pressure coefficient, p_f/q , where q is the stream dynamic pressure.

Combining equations (1) and (2) gives

$$u_U = U \sqrt{1 - P_f} + \Delta u \quad \frac{u_U}{U} = \sqrt{1 - P_f} + \frac{\Delta u}{U} \quad (3)$$

$$u_L = U \sqrt{1 - P_f} - \Delta u$$

The pressures on the upper and the lower surfaces of the airfoil at x are then, respectively,

$$\left. \begin{aligned} p_U &= q - \frac{\rho u_U^2}{2} = q - \frac{\rho}{2} (U \sqrt{1 - P_f} + \Delta u)^2 \\ p_L &= q - \frac{\rho u_L^2}{2} = q - \frac{\rho}{2} (U \sqrt{1 - P_f} - \Delta u)^2 \end{aligned} \right\} \quad (4)$$

Now, if p is the normal force experienced by the airfoil at x , then, an upward force being considered positive,

$$p = - p_U + p_L$$

Then substituting equations (4), canceling, and rearranging gives

$$p = 2\rho U \Delta u \sqrt{1 - P_f}$$

Hence

$$\Delta u = \frac{\frac{1}{4} \left(\frac{p}{\rho} \right) U}{\sqrt{1 - P_f}} = \frac{\frac{1}{4} P U}{\sqrt{1 - P_f}} \quad (5)$$

Substituting equation (5) in (4) and rearranging gives

$$\left. \begin{aligned} P_U = \frac{p_U}{q} &= 1 - \frac{\left(1 - P_f + \frac{1}{4} P\right)^2}{(1 - P_f)} \\ P_L = \frac{p_L}{q} &= 1 - \frac{\left(1 - P_f - \frac{1}{4} P\right)^2}{(1 - P_f)} \end{aligned} \right\} \quad (6)$$

Thus, if the normal-force distribution over an airfoil P and the pressure distribution over the base profile P_f are known, then pressure coefficients for the upper and the lower surfaces may be calculated.

ACCURACY AND LIMITATIONS OF THE METHOD

At the outset, it is necessary to justify the assumptions made in the development of the present method. To this end, the theoretical pressure distributions over the N.A.C.A. 4412 airfoil section at two angles of attack were calculated by the method of reference 1 and are plotted in figures 1 and 2. The theoretically exact normal-force distributions were determined from the pressure distributions for each case. The pressure distribution over the base profile (N.A.C.A. 0012 at zero angle of attack) was also calculated by the method of reference 1. By means of the normal-force and the base-profile pressure distributions, the pressure distributions were then calculated by equations (6) and are plotted for comparison in figures 1 and 2. Similar calculations were made for the N.A.C.A. 6512 and 23018 at $c_l = 0$ and $c_l = 1.0$; the resulting pressure distributions are shown in figures 3 to 6. The

N.A.C.A. 6512 airfoil is representative of the more highly cambered airfoils; the N.A.C.A. 23018, of fairly thick airfoils; and the N.A.C.A. 4412, of the more commonly employed airfoils. The agreement between the theoretical distributions and those calculated by equations (6) for the several airfoils investigated is good, as shown by the distributions in figures 1 to 6.

When this method is applied to the calculation of airfoil pressure distributions, the accuracy of the calculation will depend principally on:

- (1) The accuracy of the calculation of the chordwise normal-force distribution over the airfoil.
- (2) The accuracy of the base-profile pressure distribution.
- (3) The thickness of the boundary layer over the airfoil.

The close agreement between the theoretical pressure distributions of figures 1 to 6 shows that, for airfoils of normal profile, thickness, and camber, equations (6) are sufficiently accurate. For an airfoil with a plain flap deflected through a large angle, the basic assumption that the curvature of the mean camber line is small is disregarded so that the accuracy of equations (6) is accordingly less. The same statement is, of course, true for highly cambered airfoils. Again, the assumption that the bound vorticity may be considered as distributed along the mean camber line, although it has been shown to be permissible for airfoils of normal thickness, will probably be less accurate for the thicker profiles.

For plain airfoils, the accuracy of the method for the calculation of the normal-force distribution given in reference 3 is, as a rule, well within 5 percent; for airfoils with flaps, the accuracy of the method given in reference 4 is, as a rule, within 10 percent of the true normal-force distribution.

The base-profile pressure distribution calculated by the method of reference 1 will probably be sufficiently accurate for design purposes for all base profiles in common use. The base-profile pressure distributions for the N.A.C.A. family of airfoils, as well as for the Clark Y

and the Göttingen 398, were calculated by the method of reference 1 and are given in table I.

That the thickness of the boundary layer is a factor concerning the accuracy of this method is apparent when it is seen that not only is the base profile effectively changed when the boundary layer is thickened but also that the effective shape of the mean camber line and therefore the effective position of the bound vortices are altered when the boundary layer is thicker on one surface of the airfoil than the other (as for example when the angle of maximum lift is approached). This inaccuracy, which affects the distribution of pressure between the upper and the lower surfaces of the airfoil, exists in spite of the fact that the effect of the boundary layer on the normal-force distribution is partly taken care of by the methods of references 3 and 4.

A consideration of the several factors would lead one to expect that the method would be very accurate for thin airfoils with small amounts of camber and would be less accurate for thick highly cambered airfoils and particularly for airfoils with ordinary trailing-edge flaps. That these expectations are fulfilled is shown in figures 7 to 14, where the computed and the experimental pressure distributions for several airfoils (one with a flap) are given. In every case, the normal-force distributions were determined by the methods of references 3 and 4 and the base-profile pressure distributions given in table I were used. The experimental pressure distributions over the N.A.C.A. 4412 airfoil (figs. 7 to 10) were obtained from reference 2 and those over the N.A.C.A. 23012 (figs. 11 to 14) were obtained from reference 5.

One limitation should be noted although it is of negligible importance. Equations (6) cannot be used to predict the pressure at the most forward point of the airfoil because at this point the slope of the airfoil profile is infinite and, even though the normal force approaches zero, the solution must, of course, be indeterminate at this point. The nose point should therefore be omitted from practical calculations.

CONCLUSIONS

When the base-profile pressure-coefficient distributions given in table I and the normal-force distributions computed by the methods of references 3 and 4 are used,

the pressure distributions calculated by the method of this note are adequate for most engineering purposes. The computed pressure distributions not only agree in form with experiment but the integrated normal forces and moments agree in magnitude with experiment.

Langley Memorial Aeronautical Laboratory,
National Advisory Committee for Aeronautics,
Langley Field, Va., April 3, 1939.

REFERENCES

1. Theodorsen, Theodore: Theory of Wing Sections of Arbitrary Shape. T.R. No. 411, N.A.C.A., 1931.
2. Pinkerton, Robert M.: Calculated and Measured Pressure Distributions over the Midspan Section of the N.A.C.A. 4412 Airfoil. T.R. No. 563, N.A.C.A., 1936.
3. Jacobs, Eastman N., and Rhode, R. V.: Airfoil Section Characteristics as Applied to the Prediction of Air Forces and Their Distribution on Wings. T.R. No. 631, N.A.C.A., 1938.
4. Allen, H. Julian: Calculation of the Chordwise Load Distribution over Airfoil Sections with Plain, Split, or Serially Hinged Trailing-Edge Flaps. T.R. No. 634, N.A.C.A., 1938.
5. Wenzinger, Carl J., and Delano, James B.: Pressure Distribution over an N.A.C.A. 23012 Airfoil with a Slotted and a Plain Flap. T.R. No. 633, N.A.C.A., 1938.

TABLE I

VALUES OF $(1 - P_f)$ FOR N.A.C.A. FAMILY OF AIRFOIL SECTIONS

| Station (percent c) | Thickness (percent c) | | | | | | | | |
|---------------------------|-----------------------|-------|-----------------|-------|-------|-------|-------|-------|-------|
| | 6 | 9 | ^a 12 | 15 | 18 | 21 | 25 | 30 | 35 |
| 1.25 | 1.118 | 1.075 | 1.008 | 0.932 | 0.857 | 0.775 | 0.699 | 0.620 | 0.573 |
| 2.5 | 1.190 | 1.232 | 1.257 | 1.250 | 1.216 | 1.170 | 1.105 | 1.061 | .982 |
| 5 | 1.219 | 1.313 | 1.395 | 1.460 | 1.505 | 1.529 | 1.543 | 1.550 | 1.553 |
| 7.5 | 1.222 | 1.330 | 1.425 | 1.513 | 1.601 | 1.675 | 1.760 | 1.828 | 1.899 |
| 10 | 1.220 | 1.330 | 1.432 | 1.534 | 1.635 | 1.737 | 1.861 | 2.000 | 2.115 |
| 15 | 1.209 | 1.316 | 1.428 | 1.536 | 1.647 | 1.760 | 1.914 | 2.106 | 2.300 |
| 20 | 1.192 | 1.298 | 1.407 | 1.518 | 1.634 | 1.749 | 1.905 | 2.106 | 2.309 |
| 25 | 1.180 | 1.277 | 1.380 | 1.490 | 1.604 | 1.715 | 1.870 | 2.070 | 2.271 |
| 30 | 1.165 | 1.256 | 1.352 | 1.453 | 1.560 | 1.667 | 1.813 | 2.001 | 2.193 |
| 35 | 1.150 | 1.233 | 1.321 | 1.413 | 1.510 | 1.603 | 1.740 | 1.905 | 2.075 |
| 40 | 1.137 | 1.210 | 1.290 | 1.372 | 1.457 | 1.540 | 1.656 | 1.805 | 1.958 |
| 45 | 1.122 | 1.189 | 1.256 | 1.328 | 1.401 | 1.473 | 1.570 | 1.702 | 1.835 |
| 50 | 1.109 | 1.167 | 1.225 | 1.288 | 1.351 | 1.410 | 1.492 | 1.605 | 1.711 |
| 55 | 1.094 | 1.146 | 1.195 | 1.248 | 1.300 | 1.350 | 1.417 | 1.509 | 1.597 |
| 60 | 1.081 | 1.125 | 1.167 | 1.208 | 1.250 | 1.293 | 1.343 | 1.411 | 1.484 |
| 65 | 1.070 | 1.104 | 1.138 | 1.171 | 1.202 | 1.239 | 1.279 | 1.326 | 1.378 |
| 70 | 1.056 | 1.082 | 1.107 | 1.132 | 1.157 | 1.182 | 1.211 | 1.240 | 1.271 |
| 75 | 1.041 | 1.059 | 1.074 | 1.091 | 1.105 | 1.122 | 1.141 | 1.160 | 1.180 |
| 80 | 1.021 | 1.032 | 1.041 | 1.048 | 1.053 | 1.059 | 1.069 | 1.074 | 1.085 |
| 85 | 1.002 | 1.002 | 1.001 | 1.000 | .998 | .995 | .990 | .982 | .972 |
| 90 | .981 | .970 | .955 | .941 | .929 | .911 | .890 | .860 | .829 |
| 95 | .949 | .922 | .895 | .865 | .834 | .807 | .764 | .712 | .663 |

^aClark Y; Göttingen 398.

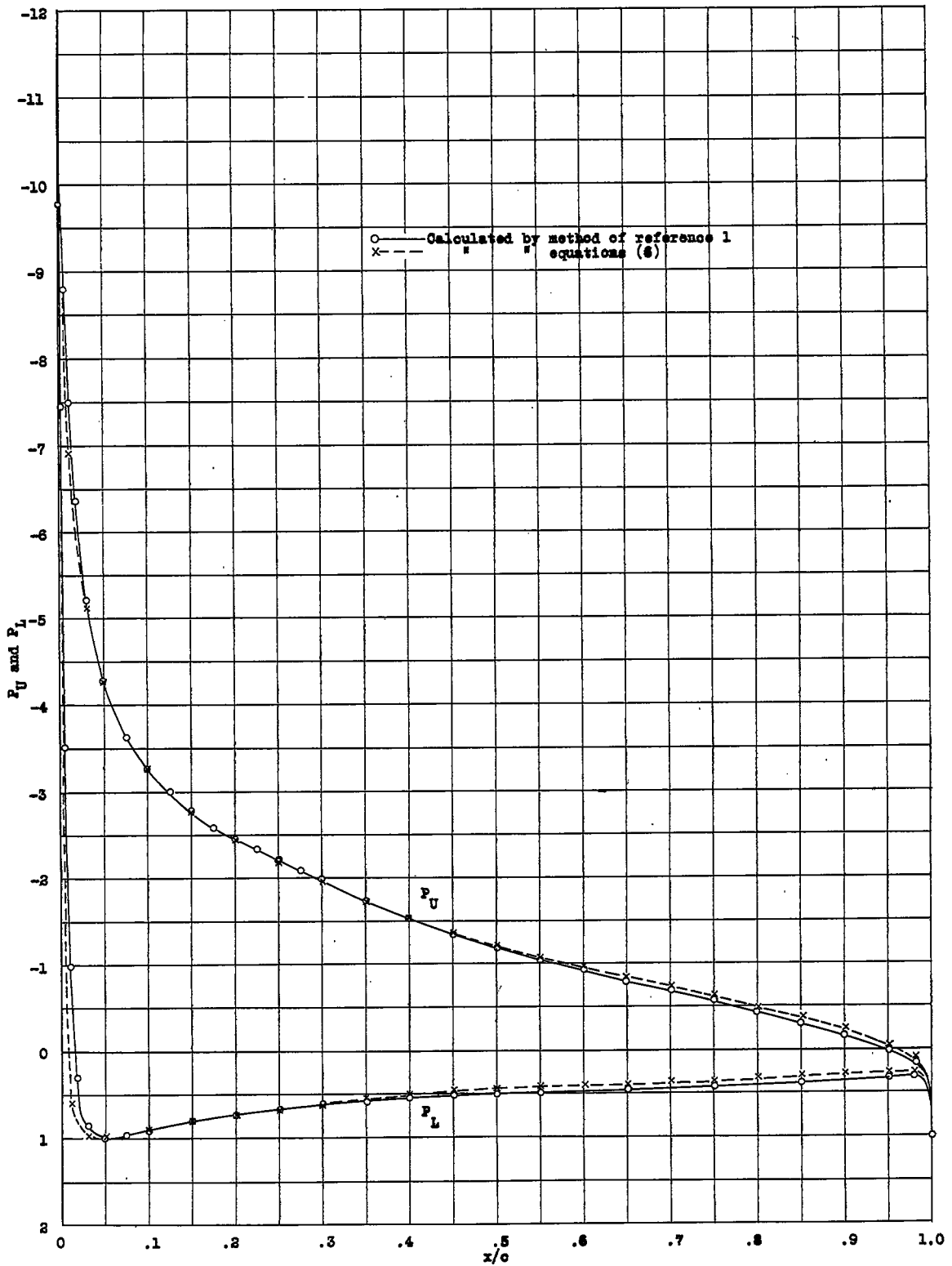


Figure 1.- Theoretical pressure distribution. N.A.C.A. 4412 airfoil; α , $15^\circ 57'$.

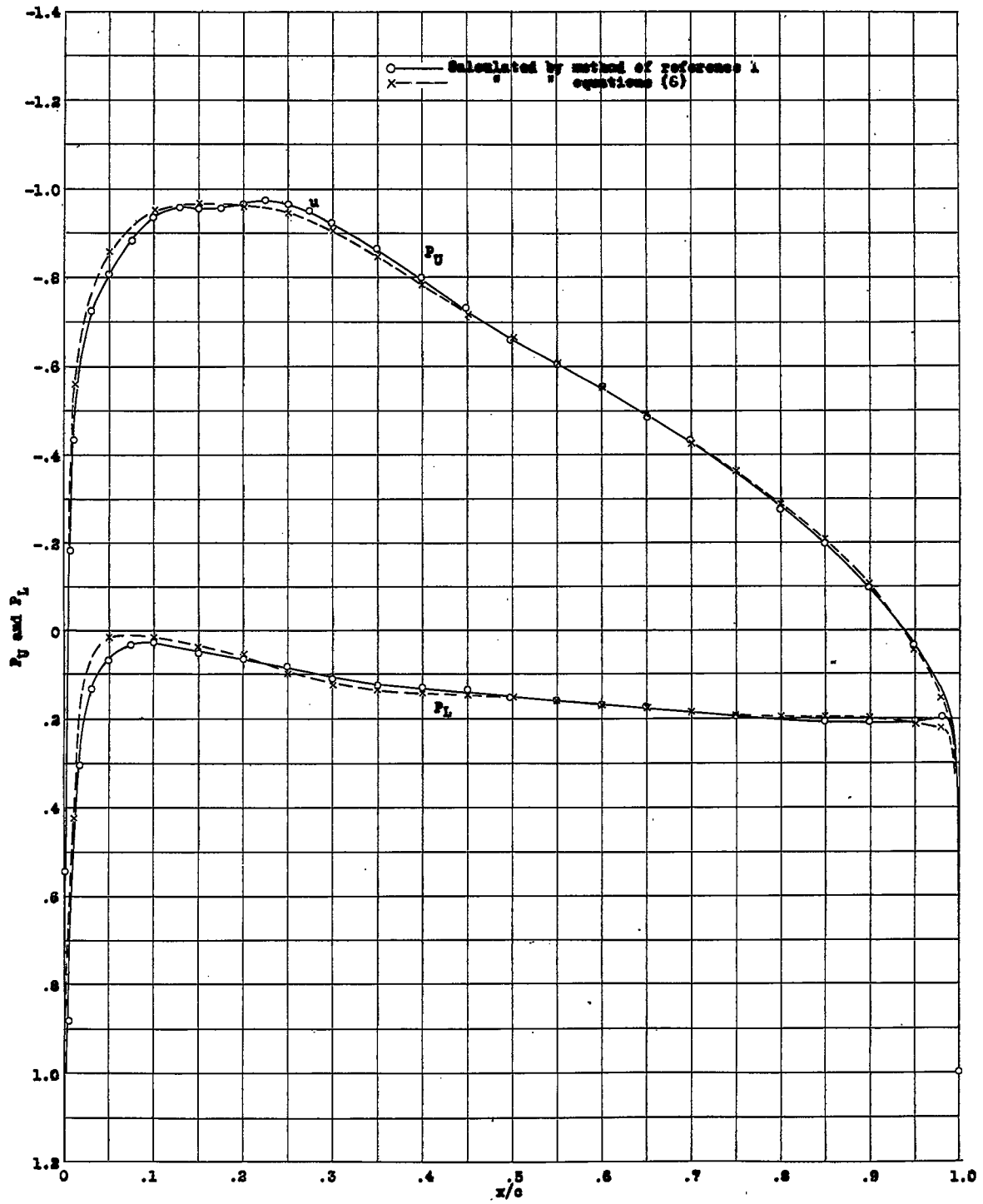


Figure 2.- Theoretical pressure distribution. N.A.C.A. 4413 airfoil; α , 2° .

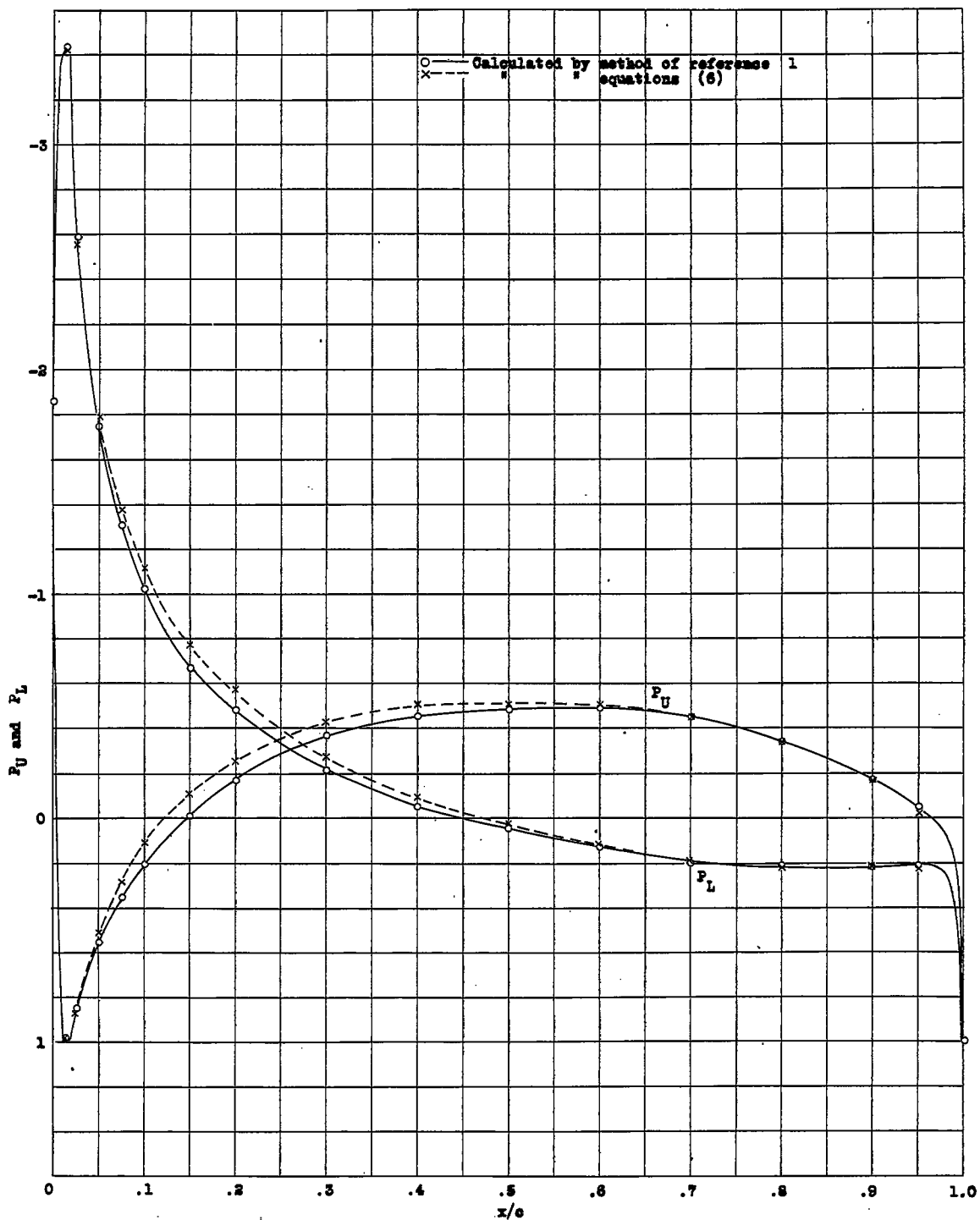


Figure 3.- Theoretical pressure distribution. N.A.C.A. 6512 airfoil; α , $-7^\circ 4'$; c_1 , 0.

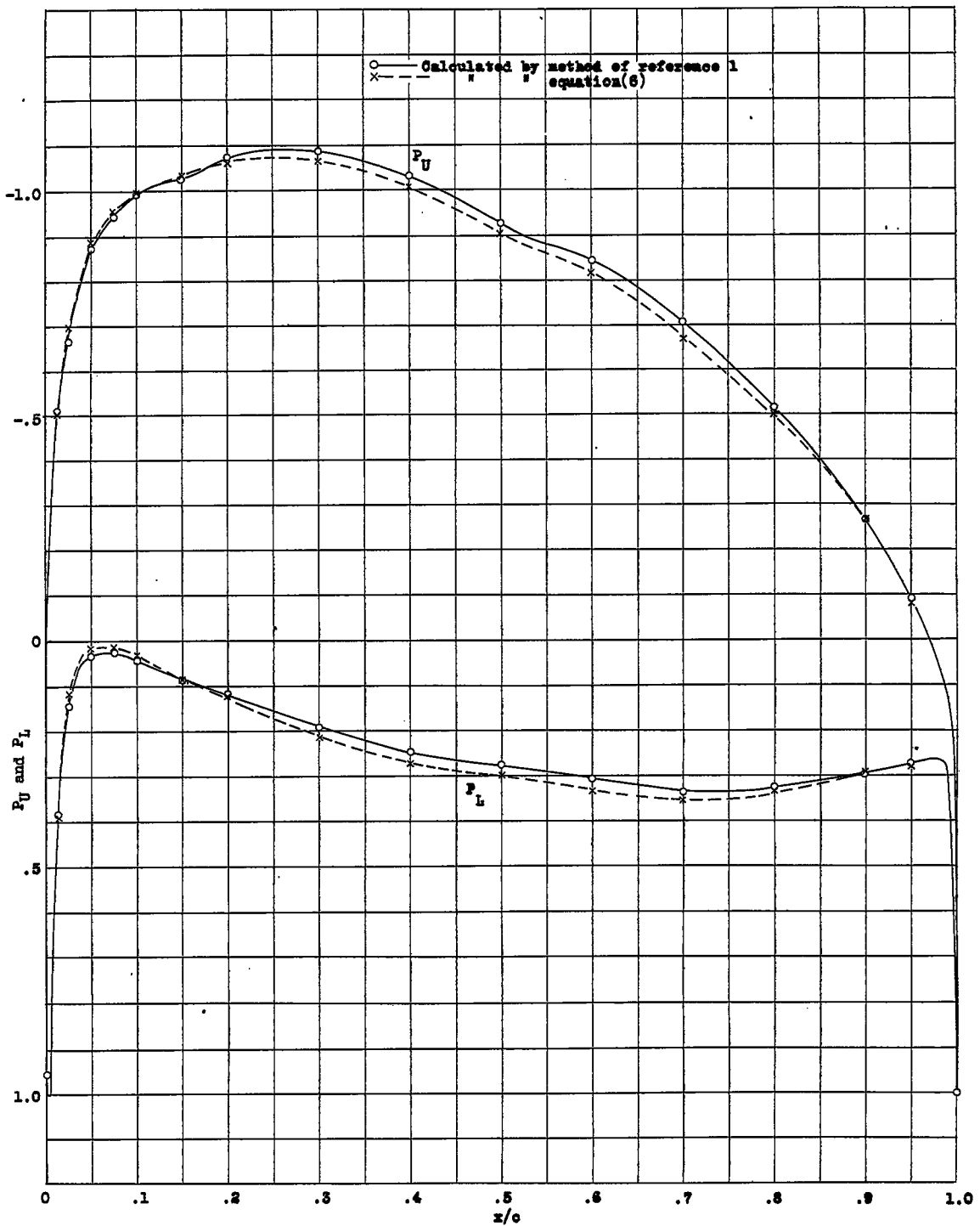


Figure 4.- Theoretical pressure distribution. N.A.C.A. 6512 airfoil; α , $1^\circ 10'$; c_l , 1.0.

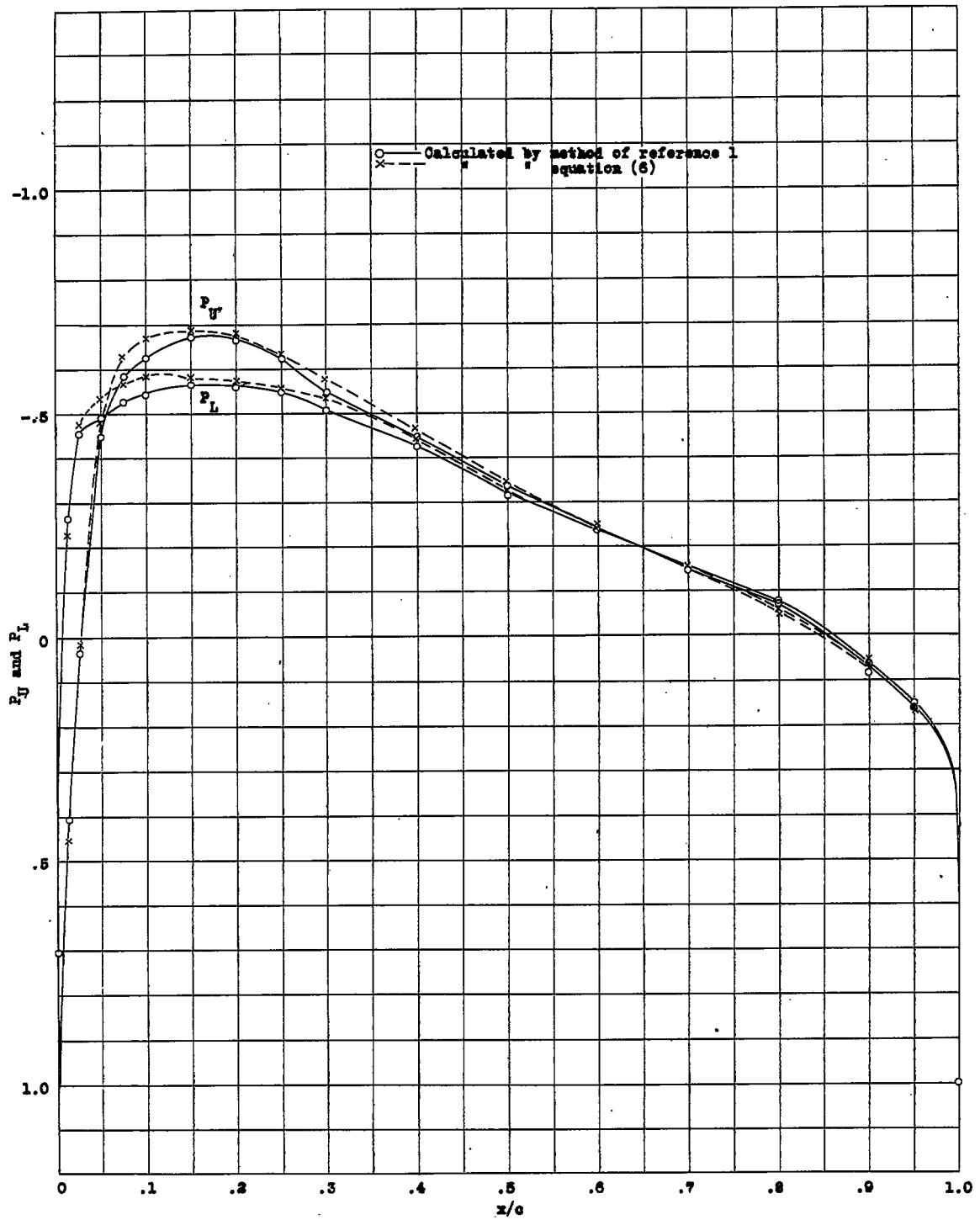


Figure 5.- Theoretical pressure distribution. N.A.C.A. 23018 airfoil; α , $-1^\circ 3'$; c_l , 0.

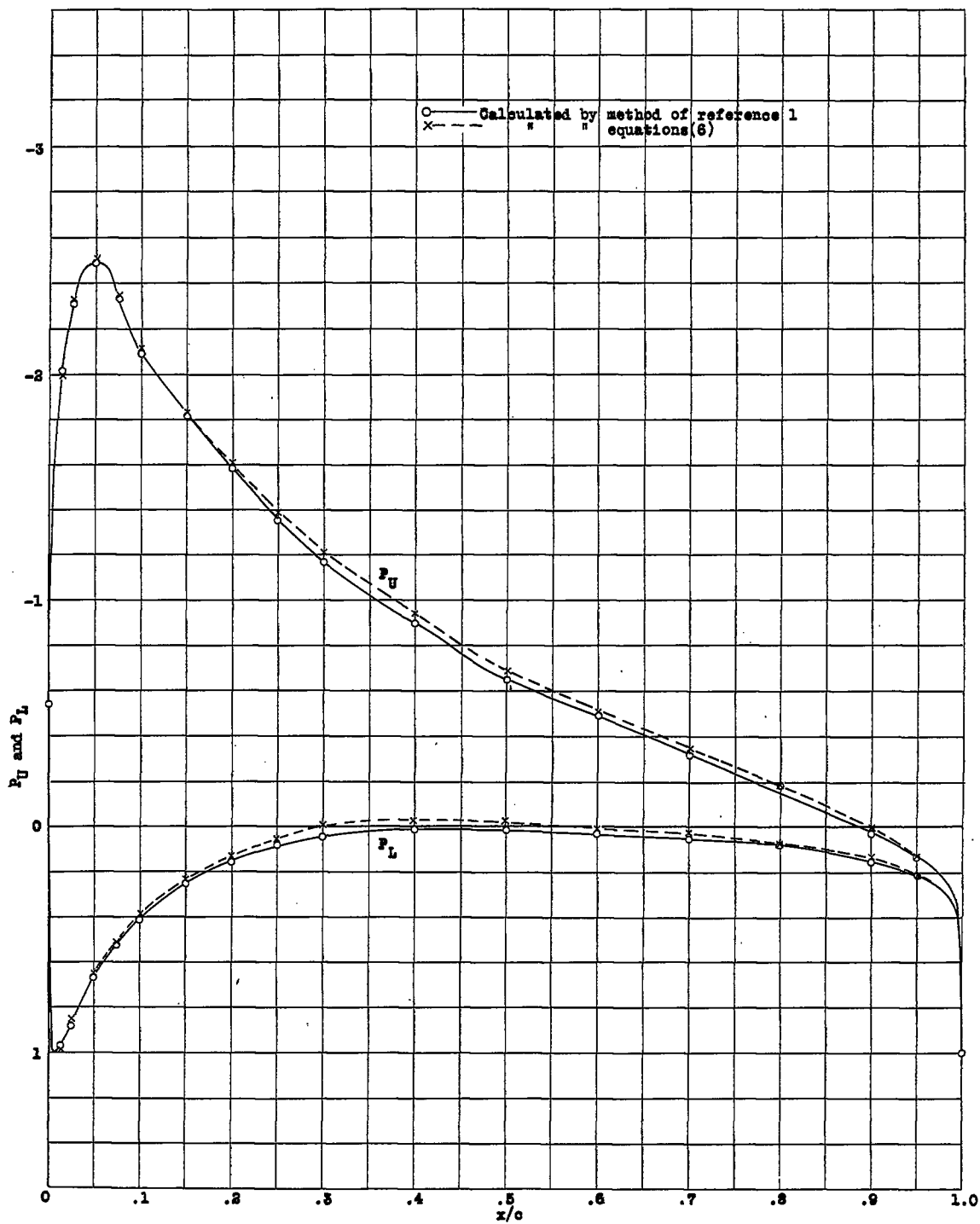


Figure 6.- Theoretical pressure distribution. N.A.C.A. 23018 airfoil; α , $6^\circ 53'$; c_l , 1.0.

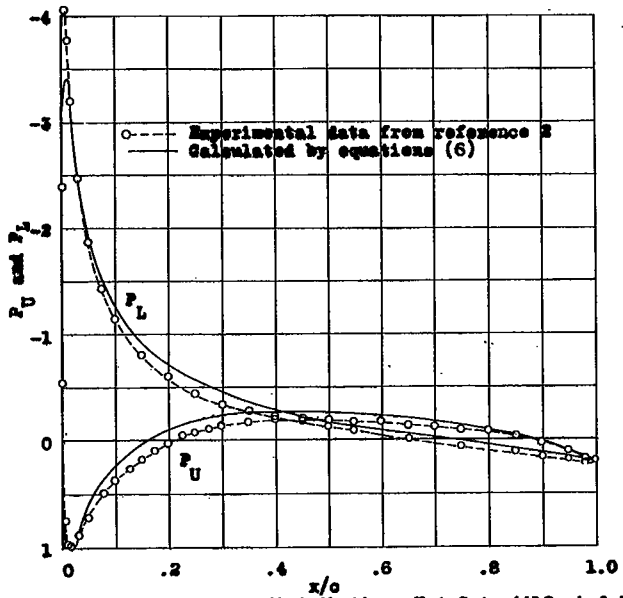


Figure 7.- Pressure distribution. N.A.C.A. 4412 airfoil; α , -3° .

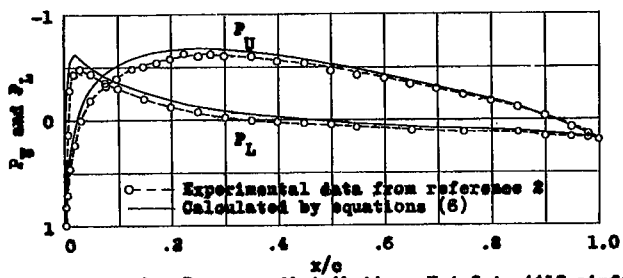


Figure 8.- Pressure distribution. N.A.C.A. 4412 airfoil; α , 0° .

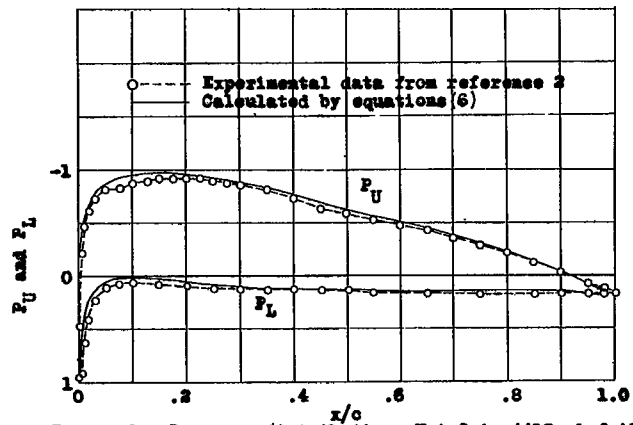


Figure 9.- Pressure distribution. N.A.C.A. 4412 airfoil; α , 4° .

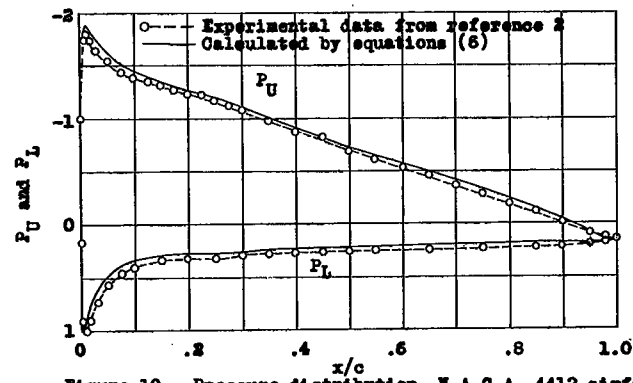


Figure 10.- Pressure distribution. N.A.C.A. 4412 airfoil; α , 8° .

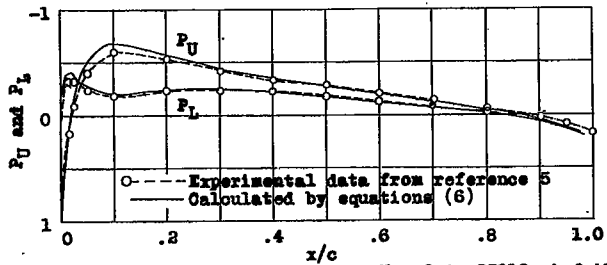


Figure 11.- Pressure distribution. N.A.C.A. 23012 airfoil with 20-percent-chord plain flap; α , 0° ; δ , 0° .

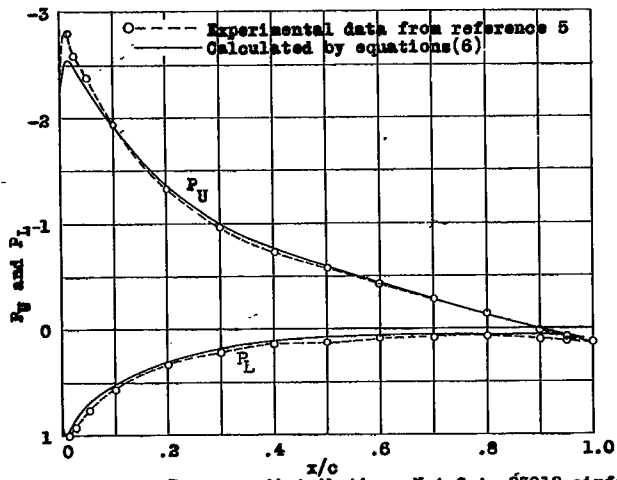


Figure 12.- Pressure distribution. N.A.C.A. 23012 airfoil with 20-percent-chord plain flap; α , 8° ; δ , 0° .

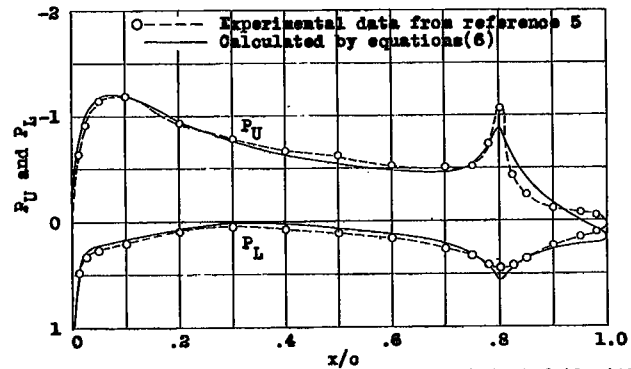


Figure 13.- Pressure distribution. N.A.C.A. 23012 airfoil with 20-percent-chord plain flap; α , 0° ; δ , 15° .

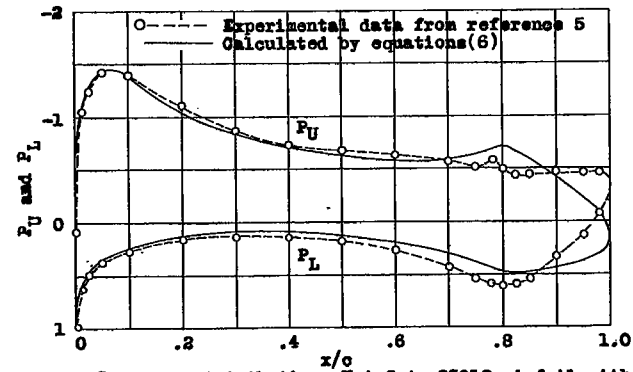


Figure 14.- Pressure distribution. N.A.C.A. 23012 airfoil with 20-percent-chord plain flap; α , 0° ; δ , 30° .